Composites Part C: Open Access 16 (2025) 100570

Contents lists available at ScienceDirect

Composites Part C: Open Access

journal homepage: www.sciencedirect.com/journal/composites-part-c-open-access

Surface tailored spent coffee ground derived carbon reinforced waste HDPE composites for 3D printing application

Sushrisangita Sahoo, Abhinav Yadav, Vijaya Rangari *

Materials Science and Engineering Department, Tuskegee University, AL, 36088, USA

ARTICLE INFO

Keywords:
Waste coffee grounds
Biocarbon
Surface modification
Plasma
Reinforcement
Sustainability

ABSTRACT

The serious impact of plastic waste on environmental pollution and climate change led to new strategies like recycle, reuse, reduce concept. This work presents a unique sustainable approach of developing filament composites with improved thermal and mechanical properties by mixing the plastic waste (i.e. waste Walmart bag, High Density Polyethylene (HDPE)) and surface engineered spent coffee ground (SCG) waste derived carbon. Carbon as filler materials were obtained by pyrolyzing the SCG waste. As the biomass derived carbon generally has inert surface properties, it causes poor compatibility between the filler and polymer matrix yielding inferior thermal and mechanical properties of the composites. So, the properties of pyrolyzed carbon in the present work were tailored by SF_6 plasma treatment at different time durations. The surface functionalization of carbon materials and optimized plasma treatment time were analyzed from different characterizations. Fourier Transform Infrared Spectroscopy (FTIR) and X-ray Photoelectron Spectroscopy (XPS) reveals 15 min plasma treatment carbon is the optimized one with highest fluorination and semi-ionic C-F bonding. Due to the highest fluorination, the I_D/I_G ratio i.e. the defect density is found to be maximum for 15 min plasma treated carbon from the Raman spectra. The 15 min plasma treated carbon with highest fluorine functionalization as a filler exhibits 33.8 % and 13.97 % improvement in tensile modulus and tensile strength in comparison to neat HDPE matrix. The feasibility test of filament composites for 3D printing suggests its application potentiality in Material extrusion (MEX) 3D printing.

1. Introduction

The multipurpose functionality of plastics in broader areas of applications such as packaging, containers, electronics and construction etc. made them an integral part of modern human life [1,2]. The basic need and convenience of modern society increases the global plastics production due to their low cost, light weight and disposability, which leads to an alarming situation of environmental pollution by plastic wastes and the greenhouse gas emissions during plastic production [3–5]. The non-biodegradable plastics wastes are either disposed to landfill or incinerated or very few like 23 % are recycled [6]. Although the recycling rate has increased nowadays, still much improvement required in this direction. During the mechanical recycling process, the physical and mechanical properties of the host polymer reduced due to chain degradation i.e. chain scission, chain crosslinking or branching caused by the shear force [7–10]. Various strategies were adopted to improve the mechanical properties of the polymer during mechanical recycling and upcycling (recovery of plastic wastes by revalorizing, reducing and reusing) process such as: (i) optimizing different parameters of melt extrusion, (ii) grafting with polymerizable monomer, (iii) addition of stabilizer and plasticizer, (iv) complex polymer blend, (iv) addition of filler etc. [11–16]. Incorporation of filler is one of the efficient ways of upcycling plastic waste, which reduces the chain degradation and improves the mechanical properties of the polymer composites. Various types of fillers such as natural fiber, glass fiber, Wollastonite, talc, $CaCO_3$, nanoparticles and inorganic fillers were incorporated to tailor different properties of the composites to fit into specific applications with a minimum processing cost [17–22]. Addition of some fillers causes deterioration of mechanical properties due to poor adhesion and interfacial interaction of the filler and polymer matrix. Cunnigham et al. reported the decrease in tensile strength with an increase in filler loading of eggshell and poultry litter ash loaded Polypropylene. Up to 10 wt% filler loading had no effect on Young's modulus, tensile strength, impact strength and flexural properties due to lack of interfacial adhesion between filler and polymer [23]. Similarly, incorporation of phosphorus and nitrogen grafted lignin and ammonium

* Corresponding author.
E-mail address: vrangari@tuskegee.edu (V. Rangari).

https://doi.org/10.1016/j.jcomc.2025.100570

Available online 21 February 2025

polyphosphate filler in high density polyethylene (HDPE) matrix lead to reduction of tensile strength and elongation at break of the composites due to poor compatibility between the filler and polymer matrix [24]. To improve the compatibility between them, some compatibilizers like maleic anhydride are added to the composites, which increase the production cost [25]. The major challenges in composites are now balancing the processing cost with optimized properties. Extensive study has been focused in this direction to resolve this problem. Utilization of biochar from agricultural, animal and food wastes as filler to any non-biodegradable or recycled plastics is the best way to reduce the negative impact of plastics on environment and valorize the waste as a resource [26–29]. Biochar as a reinforcement filler balances the gap between the production cost and composite properties. In comparison to the natural fiber, wood and other biobased fillers, biochar induces better interfacial adhesion with the polymer matrix due to its porous structure and improves the properties of the composite. As a renewable, cost-effective and sustainable filler material, biochar not only became the alternative to natural fiber and biobased fillers but also preferred as a potential substitute to other expensive carbon materials such as carbon black, graphene, carbon nanotube etc. [30,31]. This carbonaceous solid residue (biochar) can be easily obtained from the pyrolysis of any agricultural, animal and food waste in contrast to complex synthetic production methods followed for synthesis of other carbon filler materials [32]. Since biochar loading has a significant influence on the properties of the composite, a wide range of biochar loading i.e. both lower and higher loading % on different polymer matrixes were investigated in the literature. Higher percentage loading ranging from 10 to 70 wt% of rice husk derived biochar on HDPE was investigated by Zhang et al. in order to utilize a huge amount of agricultural wastes leading to environmental safety [30]. No significant change in thermal decomposition temperature was observed in the TGA analysis even after adding a wide range of biochar loading. Though the flexural strength, flexural modulus, tensile strength, and tensile modulus improved up to 50 % biochar loading, there was a decreasing trend for 60 and 70 wt% loading due to agglomeration and poor dispersion filler in the polymer matrix. Similarly, a higher percentage of biochar loading 25–35 % on polypropylene matrix causes significant reduction in ductility [33]. Whereas with only 0.5 loading % of biochar in PET, the tensile strength increased by 32 % and the tensile modulus increased by 60 % in 5 wt% of biochar reinforced PET composites [34]. Even a very lower percentage of biochar loading 0.75 wt% in polypropylene can induce an increase in tensile modulus and tensile strength by 34 % and 46 % respectively [28]. Vidakis et al. reported the filament composite of olive tree prune derive biochar/PLA composites with loading percentage of 2, 4, 6 and 8 wt%. They used those extruded filaments for 3D printing applications. The filament composite of PLA/biochar with 4 wt% exhibits optimum tensile properties [35].

However, among commonly used plastics such as polypropylene (PP), polyethylene (PE) and polyvinyl chloride (PVC), High density polyethylene (HDPE) is widely used in a broad array of applications such as in automotives, agriculture, packaging goods, machinery, toys and daily sundries due to its high mechanical strength, chemical stability, flexible, light weight, good heat resistance, and barrier properties. It is the third most used plastic in the world [31,36]. On the other hand, the dramatically increased consumption rate of coffee over the last decades is the main cause of producing large amount spent coffee ground waste (SCG) i.e. 60 million tons over a year worldwide. These abundant amounts of SCG waste having toxic content like caffeine, tannins and polyphenols are directly disposed to landfill as solid waste. The decomposition process of these SCG waste required a large amount oxygen and also releases harmful greenhouse gas like methane to the atmosphere, which is the major contributor of climate change and global warming. Therefore, an ecofriendly and sustainable valorization plan is urgently needed to channelize this waste from dumping ground into commercial applications. Transforming these SCG waste into resources is the best way to contribute towards the closed loop circular economy and resolve the environmental issues [37,38]. So, a lot of work has been reported by considering SCG waste as a bio-based filler in varieties of polymer such as polypropylene (PP), polylactic acid (PLA), natural rubber, polyvinyl alcohol (PVA) etc., but their performance was not satisfactory due to its incompatibility with most of the polymer owing to its high hydrophilic nature. So, various surface treatments of SCG were carried out to improve the interfacial interaction and consequently modifies the properties of reinforced composite [39–41]. Although SCG and surface modified SCG as bio-based filler was studied well earlier, but SCG derived biochar as filler is not properly studied as per the reported literature.

The present study covers three major areas of research i.e. from biowaste management to materials science and material extrusion 3D printing (MEX3DP) manufacturing process to obtain eco-friendly sustainable composites with improved thermal and mechanical properties. The polymer filament composites were fabricated by combining two different wastes as filler and polymer matrix, which can reduce the environmental problems and increase the sustainability of the process. Waste Walmart plastic bags made up of HDPE are used as the polymer matrix, whereas the spent coffee ground derived biochar (or carbon) used as the fillers. To improve the compatibility and interfacial adhesion between the filler and polymer matrix, plasma surface modification of the spent coffee ground derived carbon was carried out. Gautam and Mohammed et al. reported improved mechanical and thermal properties of the polypropylene and HDPE based composites reinforced with low temperature plasma treated biochar filler [42,43]. Low temperature plasma treatment became an effective technique to modify the properties of materials by surface modification and functionalization. Zhang et al. [44] reported the gas sensing behavior of fluorinated graphene by SF_6 plasma treatment. The covalent C-F bonding of the SF_6 plasma treated graphene was investigated from XPS and NEXAFS results. Again, Bulusheva et al. reported the fluorine functionalization of double walled CNT by CF_4 plasma treatment [45]. The fluorine functionalization of carbon by plasma treatment not only modify it as a good filler, it can also improvise the carbon properties for other potential applications. So, the main objective of this work focused on: (i) the synthesis of biochar/carbon from spent coffee ground waste using pyrolysis, (ii) tailoring different properties of the pyrolyzed carbon by SF_6 plasma engineering process at different plasma treatment time to get optimized functionalization, (iii) Analyzing the fluorine functionalization and optimization by correlating the results of different characterizations such as FTIR, XPS, Raman, TGA, surface micrograph and color mapping etc., (iv) incorporation of both untreated and SF_6 plasma treated biochar in waste Walmart bag polymer matrix to prepare filament composites by extrusion process, (iv) comparison of thermal and mechanical properties of the untreated and plasma treated carbon as fillers and, (v) printability test of the filament composites for 3D printing applications. The present work systematically investigated the following key results. The confirmation of fluorine functionalization by SF_6 plasma treatment from the appearance of new band in FTIR and XPS. The evidence of surface etching by plasma process from FESEM and color mapping. The defect induced by the plasma surface modification was studied from the Raman spectra. The optimization of fluorine functionalization by correlating the results of above-mentioned characterization techniques. In composites, improved thermal and mechanical properties were obtained for filament composites with the carbon having maximum fluorine functionalization. As the 3D printing of high density polyethylene are facing lots of challenges due to delamination and warpage issues, printability test of the filament composites are checked for future application purposes.

2. Experimental details

2.1. Materials

Spent Coffee Ground (SCG) waste was collected from McDonald,

Tuskegee, Alabama, USA. SCG generally contains hemicellulose, cellulose, lignin, fatty acids, polysaccharides and some minerals like Phosphorus, Nitrogen, Potassium, Magnesium, calcium, sodium etc. The Thermogravimetric Analysis (TGA) of SCG waste was carried out in the temperature range of 30–950 °C with heating rate of 10 °C/min to study the thermal degradation of all these pseudo components (cellulose, hemicellulose and lignin) as shown in Supplementary Figure S1. The major weight loss in the temperature range between 150 and 600 °C corresponds to the decomposition of main pseudo-components i.e. hemicellulose, cellulose and lignin. The thermal decomposition of other organic contents such as protein, fatty acids, polysaccharides, amino acids etc. in coffee ground waste falls in the same temperature range. [46]. This gave us a rough idea about carbonization before pyrolysis, which plays an important role in the physicochemical properties of the carbon obtained from the pyrolysis. Also, the pyrolysis temperature and conditions significantly affect the physiochemical properties like surface area, electrical conductivity, total carbon content, etc. of the obtained material. The most studied range of pyrolysis temperature for obtaining good quality and stable carbon was 600–1000 °C, because the structural changes, i.e. the rearrangement and reconstruction of carbon atoms to form graphitic layered like structure usually take place after complete carbonization [47,48]. In our case, the weight loss % of spent coffee ground (Figure S1) after 600 °C is very less, indicating the complete carbonization. The pyrolysis temperature at 800 °C was selected lower than 1000 °C to reduce the energy required during the synthesis process maintaining the sustainability prospective of the study. For the polymer matrix, waste Walmart bag i.e. high density polyethylene (HDPE) was used.

2.2. Carbon synthesis from scg

Carbon powder was obtained from pyrolyzing the spent coffee ground at temperature of 800 °C for 2 hr. with a heating rate of 5 °C/min in an autogenic high temperature pressure reactor (MTI RC—N1200 100 ml) followed by natural cooling. Then, small chunks with powder of carbon were collected from the pyrolysis chamber and dried in oven at 80 °C for 2 hr. The dried chunks were ground manually using agate mortar and pestle to get fine powder.

2.3. Surface modification by low-temperature plasma

The low temperature plasma treatment of the pyrolyzed carbon from SCG was then carried out for different time durations i.e. 5, 10, 15, 20 and 30 min using Plasma Etch PE-100 equipment in the presence of Sulfur Hexafluoride (SF_6) gas with a flow rate of 5 sccm at chamber pressure of ~0.5 Torr and RF power of 150 W. To attain uniform functionalization or surface modification, the plasma equipment is designed with a rotating tumbler. So, the carbon powder sample was placed in the rotating tumbler of the plasma equipment with a tumbler speed of 26 rpm during the plasma cycle.

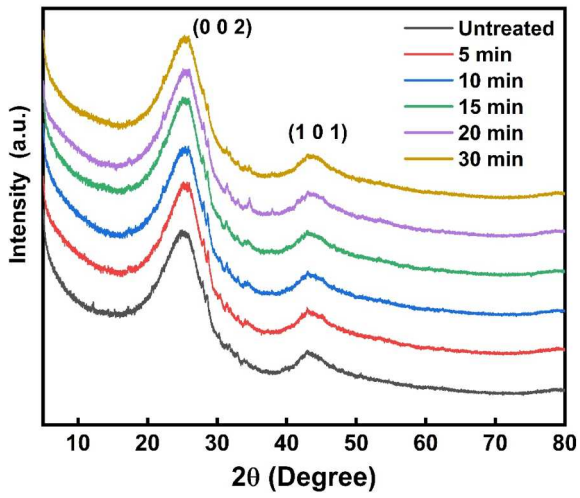

Fig. 1. XRD pattern of untreated and plasma treated carbon.

2.4. Fabrication of filament composites

For synthesis of neat polymer matrix, waste Walmart bags were collected (Walmart, Auburn, Alabama, USA) and cut into slices. Then the thin slices were extruded at 170 °C using EX2 Filabot single screw extruder. The extruded filaments are chopped into small pellet size and again extruded with the same experimental condition to get the uniform diameter filament. 2 wt% of untreated and plasma treated carbon was added to chopped pellet size neat polymer (i.e. HDPE) to make filament composites. The stoichiometric amount of untreated and plasma treated carbon was mixed manually to chopped polymer by adding two drops of polyethylene glycol as a binder. To get homogeneous dispersion of filler i.e. untreated and plasma treated carbon in the polymer matrix and uniform diameter of the filaments, all the filament composites were extruded twice in the same experimental condition. Multiple extrusion sometimes affects the properties of the filament, so the possibility of polymer chain degradation during thermal cycles is analyzed in the supplementary section through FTIR and DSC analysis. The untreated, 5, 10, 15, 20 and 30 min plasma treated carbon samples as filler in the filament composites are labelled as UTC, C-5, C-10, C-15, C-20 and C-30, respectively throughout this work.

2.5. Characterization

2.5.1. Characterization of carbon before and after plasma treatment

Structural properties of the untreated and plasma treated carbon were analyzed from the X-ray Diffraction (XRD) pattern. The XRD pattern of all the samples were recorded using Rigaku Smartlab with a Cu Kα source (λ=1.5406 Å) in the 2θ range of 10–80°, scanning rate of 1°/min and step size of 0.01. Raman spectra was obtained from Thermoscientific DXR Raman microscope with a laser of 785 nm. To verify the surface functionalization, both Fourier Transform Infrared Spectroscopy (FTIR) and X-ray Photoelectron Spectroscopy (XPS) measurements were carried out for untreated and plasma treated carbon samples. The FTIR measurement was carried out using SHIMADZU IRTracer-100 Fourier Transform Infrared Spectrophotometer in Attenuated Total Reflectance (ATR) mode with 400–4000 cm^{-1} wavelength region. To study the surface functionalization with fluorine, XPS measurement of the plasma treated carbon samples were carried out using Phi Electronics Inc. with Al X-ray source with a spot size of 100 μm and a power of 25 W. The thermal stability of fluorine functionalization of the plasma treated samples were studied from thermogravimetric analysis (TGA) curve obtained from TA Q500 instrument in an inert atmosphere with temperature range of 30–950 °C and heating rate of 10 °C/min. The surface micrographs of untreated and plasma treated carbon samples were taken using a field emission scanning electron microscope (JEOL JSM-7200F FESEM). A very few amounts of untreated and treated carbon powders were dusted above a carbon adhesive tape and the surfaces were sputtered with gold/palladium for 40 ss using Hummer 6.2 sputter coater prior to the FESEM measurement. Elemental/color mapping was obtained from the same JEOL JSM-7200F FESEM set up coupled with Energy Dispersive X-ray Spectroscopy (EDS) detector. The particle size of the pyrolyzed carbon was calculated from the surface micrograph using Image J software and the average particle size was found to be ~21 μm. The surface micrograph and the particle size distribution of SCG derived carbon was given in Supplementary Figure S2.

2.5.2. Composite characterization

To study the thermal degradation and thermal stability of the filament composites, Thermogravimetric analysis was carried out in the

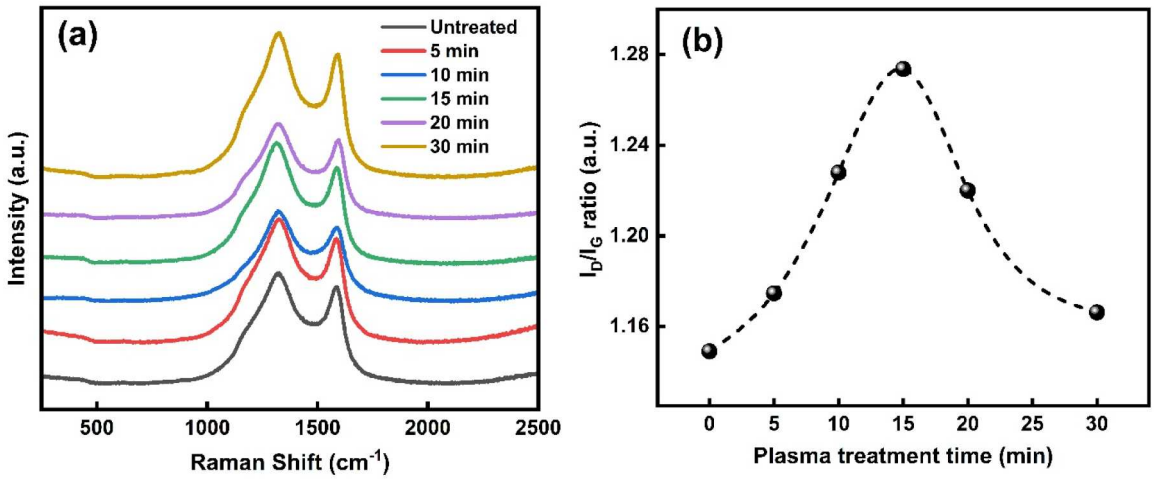

Fig. 2. (a) Raman spectra of untreated and plasma treated carbon, (b) variation of I_D/I_G ratio with plasma treatment time.

temperature range of 30–950 °C with a heating rate of 10 °C/min in the presence of nitrogen (inert) using a TA Q500 instruments. The melting, crystallization and crystallinity of the filament composites were studied from the Differential Scanning Calorimetry (DSC) curve measured using Q2000 DSC instrument with the temperature range of 30–250 °C in both heating and cooling mode. The FTIR and XRD measurement of filament composites were carried out in the same experimental conditions similar to the carbon samples and are discussed in the supplementary section. The mechanical properties of the filament composites were analyzed from the tensile test performed using a Zwick/Roell Z2.5 Universal testing machine attached with a 2.5 kN load cell. ASTM D3379 standard was followed for tensile testing of filament composites [49,50]. Five specimens of each sample were tested by keeping the test parameters as: specimen length of 100 mm, gage length of 50 mm, preload tension 0.1 N and test speed of 5 mm/min.

3. Results and discussion

3.1. Analysis of untreated and plasma treated carbon

Fig. 1 depicts the room temperature XRD pattern of untreated and plasma treated carbon for different time durations. The XRD pattern consists of two major broad peaks i.e. the peak around 25.3° and 43.17° represents the (0 0 2) and (1 0 1) planes of carbon. In general, for graphitic carbon materials, the (0 0 2) plane indicates the interlayer spacing between the carbon sheets whereas the (1 0 0) plane corresponds to the in-plane graphene network. The broad peak in our present work indicates the amorphous nature of the carbon material. In general, XRD pattern of the fluorinated carbon varies with the fluorination method (such as direct fluorination indirect fluorination, or plasma fluorination), time and the type of carbon materials. In some cases, the bulk fluorination is generally characterized by broadening of (0 0 2) planes indicating the increase in disorder due to diffusion of the fluorine in the bulk structure, which also depends upon the fluorination time and conditions. While in other cases new peak emerged around 10–15° indicating the formation of fluorocarbon lattice. As reported in Gupta et al., those broad peak at around ~18° indicates the intercalated C_xF phase of sp^2 hybridization [51]. In our plasma treated carbon materials, we did not observe any shifting in (0 0 2) plane position, but the FWHM slightly decreases (such as 0.13° for 15 min plasma treated carbon) indicating the increase in crystallite size or apparent stack size L_c (0 0 2). The narrowing of peak with decrease in FWHM and the unchanged position of (0 0 2) plane also suggests the change in the turbostratic graphitic structure (i.e. the less ordered graphitic phases) of the carbon material [52].

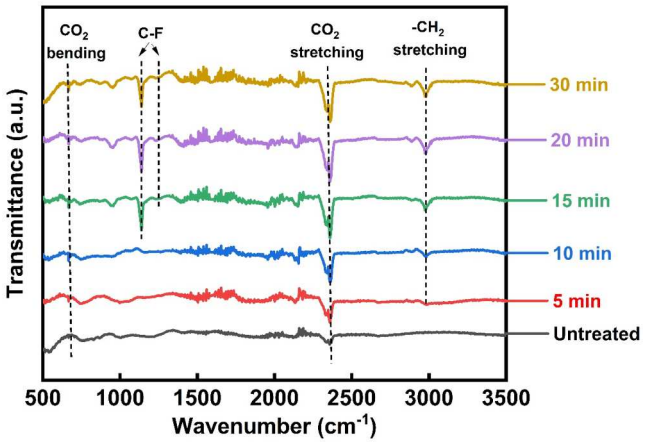

Fig. 3. FTIR spectra of untreated and plasma treated carbon.

The Raman spectra of untreated and SF_6 plasma treated carbon at different durations are shown in Fig. 2(a). Both the untreated and plasma treated carbon exhibits the two characteristics band of amorphous graphitic structure. For untreated carbon, the defect induced peak called d-band appeared at ~1318 cm^{-1}, whereas the peak corresponds to the ordered graphite called G-band with $E_{2\ g}$ symmetry observed at ~1587 cm^{-1}. The d-band remain almost unchanged with the plasma treatment from 5 min to 30 min, but the G band blue shifted from 1587 to 1592 cm^{-1} after 10 min plasma treatment similar to the reported literature. Zhang et al. [44] reported the blue shift of the G-band with increase in plasma treatment durations for SF_6 plasma treated graphene samples and the shifting was correlated with the formation of covalent C-F bond. They mentioned the peak shifting towards higher wavenumber/frequency agrees well with the p-type doping assisted blueshift induced by the strong electron withdrawing capability of fluorine. The blue shift of the G-band was also reported for Li^{3+} intercalated synthetic graphite during the initial stage of intercalation phase formation due to the increase in force constant of sp^2 hybridized carbon bond in periodically arranged graphite lattice [53]. So, the blue shift after 10 min plasma treatment time in our work attributed to the formation of intercalated phase and C-F bonding (investigated in the next sections). To study the influence of plasma treatment time on our carbon material, we have calculated the I_D/I_G ratio to estimate defect density. I_D/I_G ratio increases with increase in plasma treatment time, found to be maximum for 15 min and then decreases as shown in Fig. 2(b). During the plasma treatment, the fluorine atoms interact with the carbon to form either

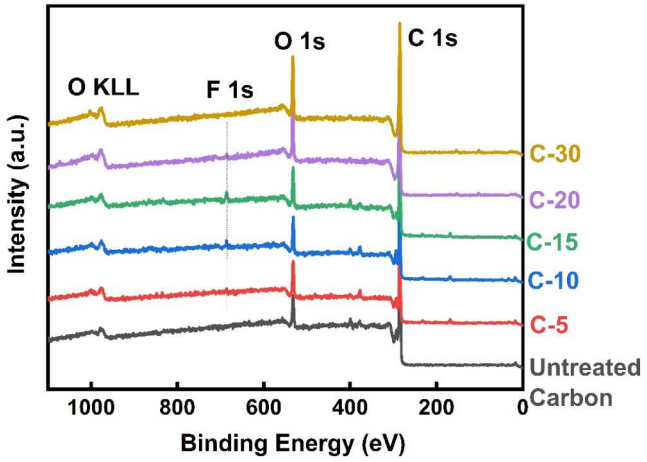

Fig. 4. XPS spectra of untreated and plasma treated carbon.

intercalated phase in between the graphitic layer or covalent bonding or some of them might be physically absorbed in the surface, which results some defects in the structure and increase in I_D/I_G ratio. But further plasma treatment after an optimized time (let say 15 min) causes breakdown of C-F bonding formed earlier, releases the F atoms from the structure in a systematic manner and rebuilt the earlier structure i.e. C=C bonds. The C-F bond breaking also depends on the nature of the bonding whether semi-ionic or covalent due to their different chemical environment or structural arrangement, the semi-ionic one can easily breakable in comparison to the covalent one.

Fig. 3 shows the FTIR spectra of untreated and SF_6 plasma treated carbon at different durations. The band at 2979 cm^{-1} for all the plasma treated carbon materials corresponds to the symmetric stretching band of -CH_2. The band at around 2358 cm^{-1} and 667 cm^{-1} represents the asymmetric stretching band and bending modes of -CO_2 respectively. FTIR study provided the first insight of C-F bond i.e. the strong band appeared at 1138 cm^{-1} for 15, 20- and 30-min plasma treated carbon. The C-F bonding in carbon materials is mainly categorized into covalent and semi-ionic type. The former one generally observed in the higher wavelength region i.e. 1220 cm^{-1}, whereas the IR band of the later one appeared in relatively lower wavelength region i.e. at 1150 cm^{-1}. The semi-ionic type, the C-F bonds were linked in the coplanar carbon atoms in the weekly fluorinated region [54]. This indicates that the band observed for 15 min, 20 min and 30 min plasma treated carbon is of semi-ionic type. In addition to that strong band, a small hump corresponding to the covalent C-F bond also obtained at around 1220 cm^{-1}. As reported in the literature, the covalent and semi-ionic C-F bonding nature can be differentiated from both the FTIR and XPS spectra, beside that their thermal stability/ thermal decomposition temperature also obtained at different temperatures due to their different chemical environment mainly the structural arrangements. The thermal decomposition temperature corresponding to the semi-ionic bonding observed at around 250 °C, whereas the covalent bonded C-F bonding have the higher decomposition temperature i.e. 450 °C. To further verify C-F bonding nature, we studied both the TGA and XPS analysis in our next section.

Fig. 4 shows the stacked XPS spectra of untreated and plasma treated carbon. The existence of F 1s peak in the plasma treated samples confirms the successful fluorination of the carbon samples. The C 1s and F 1s peak are deconvoluted to understand C-F bonding characteristics. The deconvoluted C 1s spectra of 15, 20- and 30-min plasma treated carbon (i.e. C-15, C-20 and C-30) are shown in Fig. 5 (a, b, c). The peak at binding energy ~284.5–285.2 eV represents the C—C or C = C i.e. sp^2/sp^3 carbon. The peak centered at 285.65 eV, 286.89 eV, 288.5 eV and 291.7 eV in C 1 s spectra of 15 min plasma treated carbon represents the C—CF, C—CF_2, C-F, C-F_2 respectively [44]. For 20 min plasma treatment, the C—CF peak disappears, the contribution from C—CF_2 peaks reduced from 8.8 % to 7.76 % and the sp^2/sp^3 carbon contribution increased from 67.28 % to 74.49 %. Finally, the C-F_2 peak disappears in addition to the C—CF peak along with an increase in sp^2/sp^3 carbon contribution to 80.53 % for furthermore plasma treatment i.e. 30 min. This agrees well with systematic decrease of I_D/I_G ratio in Raman analysis. This further confirms that up to an optimized plasma treatment duration i.e. 15 min, the fluorine bonded with carbon in different manner with reduction of C = C contribution, then further plasma fluorination breaking down those previously formed bonds, removing out the fluorine atom with reduction of fluorine content and rebuilding

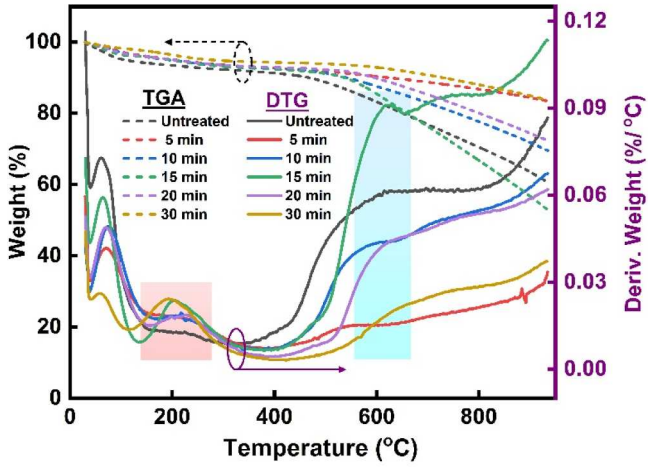

Fig. 6. TGA and DTG curve of untreated and plasma treated carbon.

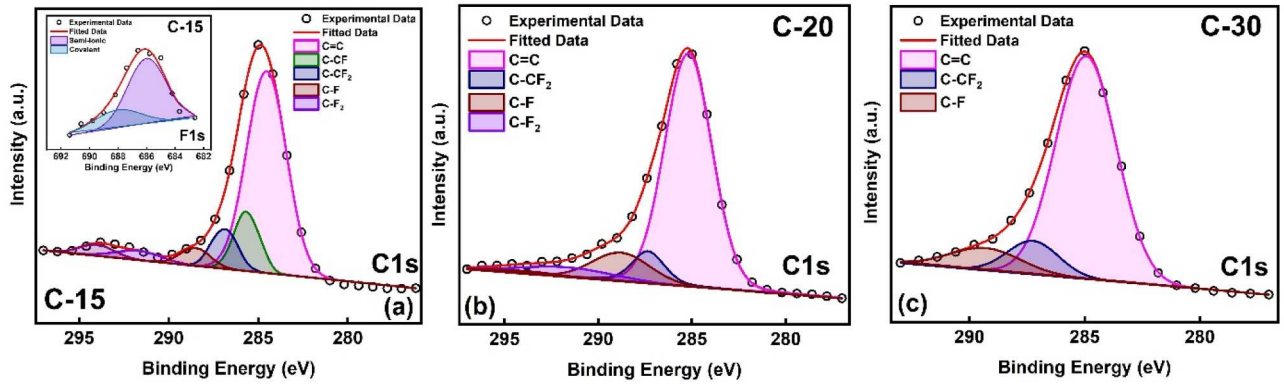

Fig. 5. Deconvoluted C 1 s spectra of (a) 15 min, (b) 20 min and (c) 30 min plasma treated carbon.

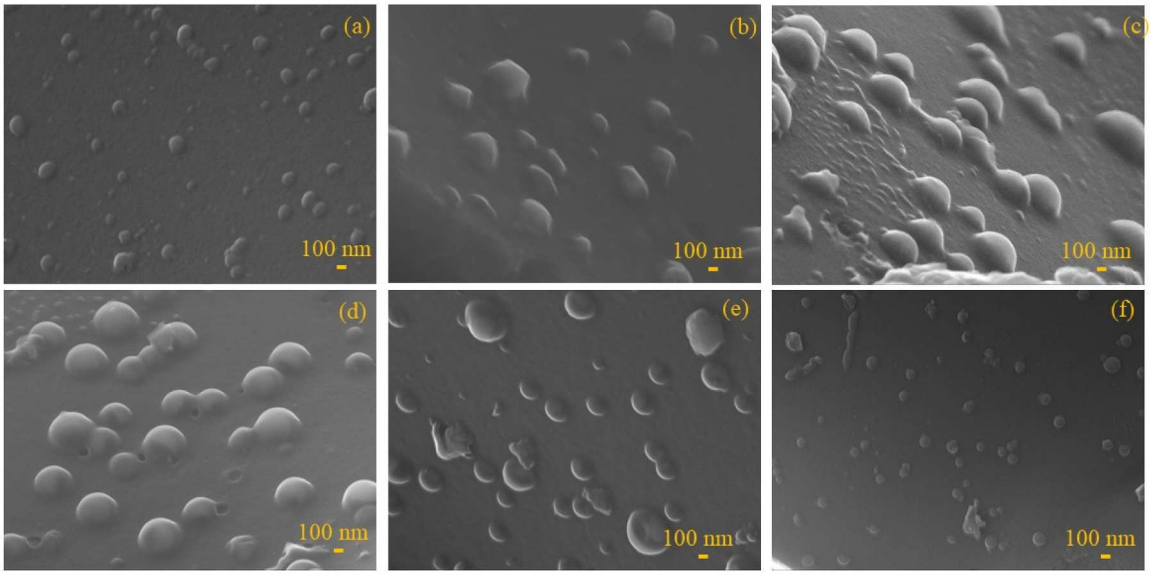

Fig. 7. Surface micrograph of (a) untreated, (b) 5 min, (c) 10 min, (d) 15 min, (e) 20 min, (f) 30 min plasma treated carbon.

the earlier structure with increase in C=C contribution. This result is also accompanied by the reduction of F 1 s spectra after 15 min plasma treatment. Inset of Fig. 5 (a) shows the F1 s spectra of 15 min plasma treated carbon. The peak in the higher binding energy around ~688.5 eV corresponds to the covalent C-F bond and the peak in the lower binding energy indicates the semi-ionic C-F bonding. The dominance of semi-ionic C-F bonding corelates well with the strong band of 1150 cm^{-1} in the FTIR results.

Again, it was reported that the thermal stability of covalent C-F bond is superior than the semi-ionic type and the bond generally breaks above 400 °C, whereas the semi-ionic bond can break at relatively lower temperature around ~250 °C due to its different chemical environment i.e., different structural arrangement of carbon atom compared to the covalent bonded one [54,55]. The peak at around ~210 °C in the derivative wt% plot (Fig. 6) confirms the thermal decompositions of semi-ionic C-F bond in the plasma treated samples. It is clear from the figure that for untreated carbon there is no peak in that region confirming the successful fluorination of carbon sample after plasma treatment. The thermal decompositions of untreated carbon after 400 °C may be due to the degradation of some volatile carbon compounds and thermal decompositions of uncharred lignin component which could not fully decompose during the pyrolysis of 850 °C as its thermal decomposition range is broad (from 150 to 900 °C) [56]. This thermal decomposition temperature shifted to higher temperature after the plasma treatment. The highest weight loss and shifting of thermal decomposition temperature to higher temperature in 15 min plasma treated carbon attributed to the breaking of covalent bond. The reduction of covalent bond content and disappearance of other fluorine bonded carbon along with the increase in C=C bond systematically reduce the mass loss and increase the thermal stability of 20 and 30 min of plasma treated carbon. The systematic trend of weight loss is directly connected to the evolution and disappearance of different fluorine bonded species with carbon during plasma treatment.

The effect of plasma treatment on surface morphology was studied from the FESEM image in the same magnification (as shown in Fig. 7 (a-f)). The bump structure on the surface of the carbon particle grows larger and became more intense up to the optimized plasma treatment time (15 min) and became smaller eventually with further plasma treatment. The bump structures in the surface may be originated during the interaction of highly reactive fluorine atoms/ions with carbon structure to form bonding or etching. Similar bump structures were also observed in SF_6 plasma treated hemp-derived carbon and direct fluorinated carbon fibers [42,57]. To further confirm the origin of bump structure from fluorine, we did the color elemental mapping of the samples as shown in Fig. 8. In Fig. 8(a), for 15 min plasma treatment sample, white things observed on the surface are mainly fluorine (shown in green spots for fluorine elemental mapping) and on that particular region there is lowest count of carbon clearly indicating the effective etching of the

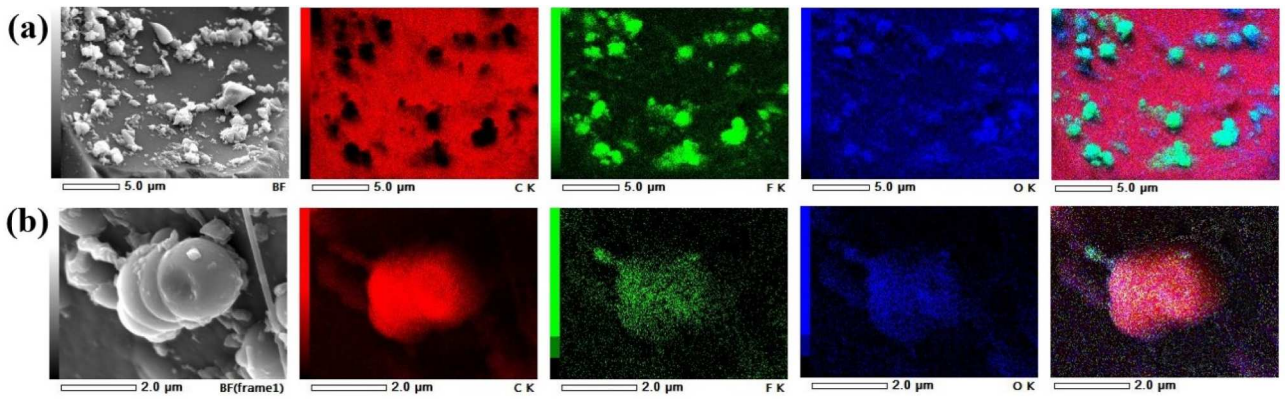

Fig. 8. (a, b) Elemental mapping of 15 min plasma treated carbon.

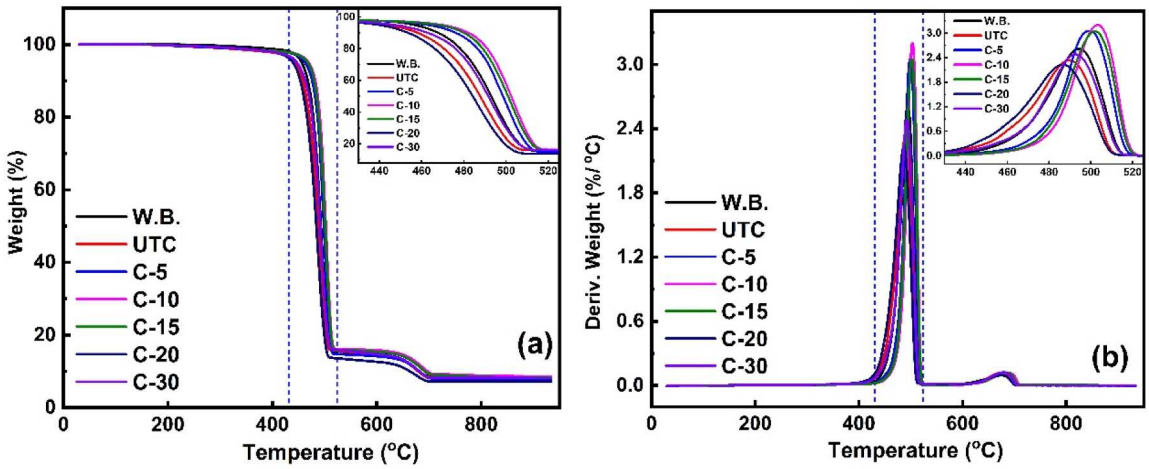

Fig. 9. TGA graph of filament composites (a) weight % and (b) derivative wt% with temperature.

surface material. For the same 15 min plasma treatment sample in different region with the bump structure was analyzed with color mapping as shown in Fig. 8(b). In that region, both the carbon and fluorine are present indicating the C-F functionalization/bonding.

3.2. Effect of untreated and SF_6 plasma treated carbon filler on hdpe

3.2.1. Thermal properties of filament composites

To study the effect of untreated and plasma treated carbon filler on the thermal properties of HDPE polymer matrix, both TGA and DSC measurements were carried out. The variation of weight% and derivative wt% for all the filament composites were shown in Fig. 9 (a, b). The thermal degradation of the neat polymer (waste Walmart bag) started at around 474 °C and maximum degradation occurred at 494 °C with weight loss of around 85 %. When the untreated carbon incorporated to the neat Walmart bag (i.e. HDPE) polymer matrix, the initial thermal degradation and maximum degradation temperature decreased to 467 °C and 490 °C respectively. The reduction of thermal degradation temperature is attributed to the weak adhesion and lack of compatibility between the untreated carbon filler and polymer matrix. However, the thermal degradation temperature increased for 5, 10 and 15 min plasma treated carbon. The initial thermal degradation temperature delayed by 13 °C and 11 °C in comparison to neat polymer for 10- and 15-min plasma treatment carbon as filler, whereas there is around 20 and 18 °C delay in comparison to untreated carbon as filler. This clearly indicates that the effective surface functionalization of carbon by fluorine groups through plasma treatment improves the interaction between the filler and polymer matrix and hence the enhancement of thermal stability of the filament composite. The increase in thermal stability after surface modification by NaOH and silane chemical treated hemp fiber reinforced HDPE composites were reported in the literature. They mentioned that the increase in thermal stability attributed to the bond formation and changes made due to surface modification by these chemical treatment on hemp fiber. The attached functional groups due to these chemical surface modifications coupled with HDPE polymer matrix and increased the physical compatibility [58]. The reduction in different fluorine species for 20 and 30 min plasma treated carbon yields reduction in thermal degradation temperature of the composite having them as filler. The decrease in thermal degradation temperature in C-20 and C-30 as filler less than the neat WB polymer matrix is attributed to the catalytic effect of these biochar particles. The reduction of thermal stability due to the catalytic effect of coffee ground based biochar on neat PLA matrix was also reported earlier [59]. After the optimized fluorine functionalization by SF_6 Plasma treatment, further plasma treatment created some active sites due to reduction of fluorine species and alternation of other functional groups in the carbon surface. The catalytic effect on thermal degradation was also observed for untreated carbon as filler. The initial thermal degradation temperature (onset temperature), maximum thermal degradation temperature (maximum rate of decomposition) and the residue after the major degradation were listed in Table 1. An additional decomposition observed in the TGA graph at temperature range of 630–700 °C similar to the reported literature [60]. This additional thermal degradation was attributed to the inorganic additive (generally calcium carbonate) added to the plastic bags during the production process. The existence of calcium carbonate was analyzed in the supplementary section through XRD, FTIR and EDS of the filament composites. The residue after second thermal degradation i.e. after 700 °C was also listed in Table 1.

Table 1
Thermal degradation parameters from TGA analysis.

Filament sample name	Initial thermal degradation temperature (onset temperature)	Maximum thermal degradation temperature (max. rate of decomposition) from peak position of Deriv. wt%	Residue (%) after first major thermal degradation	Residue (%) after 700 °C
WB	474	494	15.42	8.56
UTC	467	490	15.01	8.37
C-5	483	499	14.39	7.72
C-10	487	503	16.01	8.60
C-15	485	502	15.70	7.41
C-20	462	487	13.21	7.24
C-30	472	492	14.89	8.13

Fig. 10 shows the melting and crystallization behavior of the filament composites obtained from DSC analysis. The melting temperature, melting enthalpy, crystallinity and crystallization temperature of all the filament composites samples were listed in Table 2. The melting temperature of the neat Walmart bag HDPE polymer matrix is observed at 133.1 °C. There is no significant change in the melting temperature was observed when untreated carbon was added as the filler in the neat polymer matrix. But, the melting temperature shifted slightly to the lower temperature side (around 1.3 °C except C-20) for all the plasma treated carbon as filler indicating the interaction filler with polymer matrix after effective functionalization or surface modification by fluorine atom. The surface modified carbon filler disrupts the long chain order of polymer matrix, resulting a reduction in melting temperature [61]. Since crystallinity of the samples plays an important role in the mechanical properties of the polymer composites, we calculated the crystallinity using the following formula:

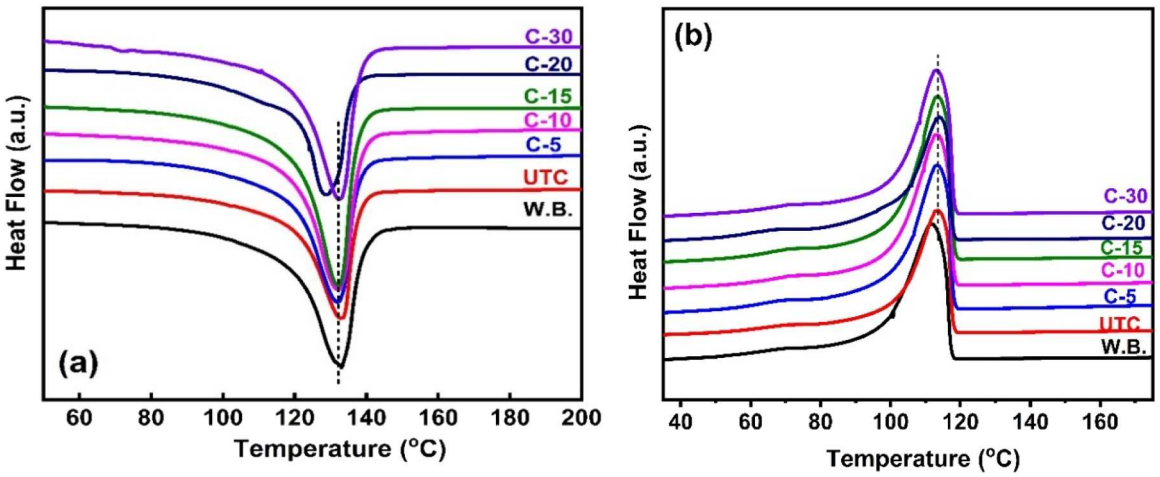

Fig. 10. DSC curve for filament composites (a) melting and (b) crystallization behavior.

Table 2
Melting and crystallization parameters obtained from DSC analysis.

Filament sample name	Melting temperature (°C)	Melting enthalpy (ΔH_m in Jg^{-1})	Crystallinity (χ_c)	Crystallization temperature (°C)
WB	133.1	98.07	34.15	111.5
UTC	132.9	118.9	41.41	113.4
C-5	131.8	130.6	45.48	113.3
C-10	131.8	131	45.62	113.2
C-15	131.8	130.4	45.41	113.4
C-20	128.6	107.1	37.29	113.9
C-30	131.8	134.7	46.91	113.1

$$\chi_c = \frac{\Delta H_m}{\varphi \times \Delta H_{m100}}$$

ΔH_m = measured enthalpy

ΔH_{m100} = 100% crystalline HDPE $(293\ Jg^{-1})$

φ = wt% of polymer

The crystallinity increased after adding both untreated and plasma treated carbon as filler due to interaction of filler with the polymer matrix. The crystallization temperature of untreated and plasma treated carbon incorporated waste Walmart bag polymer matrix is found to be higher than the neat Walmart polymer matrix. No significant changes in the crystallization temperature was observed for untreated and plasma treated carbon as filler. But the crystallization enthalpy was found to be higher in plasma treated carbon as filler than the untreated carbon. The filler particles act as nucleating site, so when the waste Walmart polymer matrix cools the nucleation occurs in the filler surface yielding a higher crystallization temperature than the neat polymer [62].

3.2.2. *Tensile properties of filament composites*

The influence of untreated and plasma treated carbon from spent coffee ground waste as filler on the mechanical properties of waste Walmart bag HDPE filament were investigated from the tensile test as shown in the Fig. 11 (Stress-Strain Plot) and the mechanical testing

Table 3
Tensile test results of filament composites.

Filament composite samples	Tensile Modulus (GPa)	Tensile strength (MPa)
WB	0.34±0.03	19.74 ± 0.69
UTC	0.21±0.1	18.62 ± 0.28
C-5	0.28 ± 0.11	21.35 ± 0.05
C-10	0.33 ± 0.04	21.14 ± 0.39
C-15	0.45±0.03	22.5 ± 0.77
C-20	0.26±0.1	19.52 ± 0.3
C-30	0.31 ± 0.02	21.07±0.6

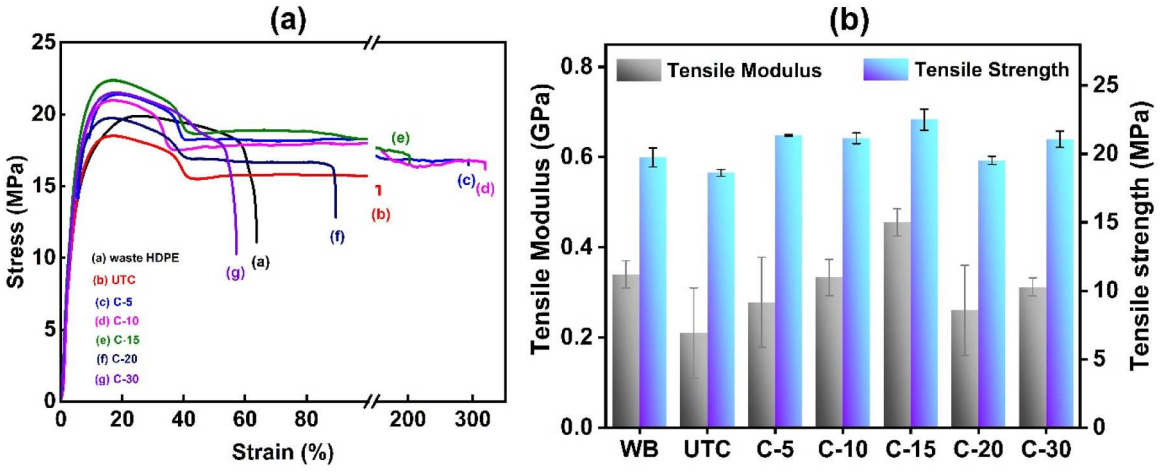

Fig. 11. (a) Stress-Strain behavior of filament composites, (b) average value of tensile modulus and tensile strength with standard deviation.

Table 4
The comparison of thermal and mechanical properties of thermoplastics filament composites with this work.

Polymer Matrix	Filler	Filler content wt %	Effect of biochar addition on		Ref.
			Thermal properties	Mechanical properties	
PLA	Olive tree pruning derived carbon	2, 4, 6, 8	Both T_{onset} and T_{max} decreased than the neat polymer.	4 wt% loading shows improvement of 17.3 % in tensile modulus and 19.5 % in tensile strength.	[35]
HDPE	Glass micro balloons	20, 40, 60	–	Tensile modulus increased by 8.17, 14.40, and 46.81 % in 20, 40 and 60 wt% loading, respectively. Tensile strength decreases than the neat polymer.	[62]
HDPE	Hemp derived carbon	0.25, 0.5, 1, 2	T_{onset} delayed by 6 °C for 0.5 wt % and T_{max} delayed by 3 °C for 0.25 wt %	1 wt% loading shows improvement of 65 % in tensile modulus and 67 % in tensile strength.	[42]
HDPE	Plasma treated hemp derived carbon	0.25, 0.5, 1, 2	T_{onset} delayed by 5 °C for 2 wt % and T_{max} delayed by 2 °C for 1 wt %	1 wt% loading shows improvement of 71 % in tensile modulus and 73 % in tensile strength.	[42]
Waste HDPE	Spent coffee ground derived Carbon	2	T_{onset} and T_{max} decreased by 7 °C and 4 °C, respectively	Tensile modulus and tensile strength decreased by 38.2 % and 5.7 % respectively	This work
Waste HDPE	SF_6 plasma treated carbon at different plasma treatment time (5, 10, 15, 20, 30 mins)	2	T_{onset} and T_{max} delayed by 11 °C and 9° for 15 min plasma treated carbon as filler	15 min plasma treated carbon as filler exhibits highest improvement of 33.8 % in tensile modulus and 13.97 % in tensile strength.	This work
PP	Packaging waste derived carbon	1, 3, 5, 10	T_{onset} and T_{max} delayed by 25 °C and 11° for 10 wt%, respectively	3 wt% loading shows improvement of 28 % in tensile modulus and 30 % in tensile strength.	[28]
PP	Ultrasonicated Packaging	0.1, 0.25,	T_{onset} and T_{max} delayed by	0.75 wt% loading shows improvement	[28]

Table 4 (*continued*)

Polymer Matrix	Filler	Filler content wt %	Effect of biochar addition on		Ref.
			Thermal properties	Mechanical properties	
	waste derived carbon	0.5, 0.75, 1	51 °C and 40° for 0.75 wt %, respectively	of 34 % in tensile modulus and 46 % in tensile strength.	
Bioplast/ PLA blend	Coconut shell derived carbon	0.2, 0.6, 1	Both T_{onset} and T_{max} decreased than the neat polymer blend system.	0.75 wt% loading shows improvement of 76 % in tensile modulus and 34 % in tensile strength.	[49]

parameters are listed in Table 3. For untreated carbon as filler, both the tensile modulus and tensile strength decreased by 38.2 % and 5.7 % respectively compared to the neat polymer due to lack of proper interface between filler and polymer matrix. But the incorporation of plasma treated carbon as fillers improved the tensile strength by 8.15 % and 12.79 % for C-5 up to maximum 13.97 % and 17.24 % for C-15 in comparison to neat HDPE and filament composite with untreated carbon as filler, respectively. The tensile modulus is found to be maximum i.e. 0.45 GPa for 15 min plasma treated carbon samples as filler suggesting around 33.8 % and 53.33 % increment in comparison to neat polymer matrix and filament composite with untreated carbon as filler, respectively. The improved tensile modulus and the increased crystallinity confirm the enhanced interfacial interaction between the filler and polymer matrix after surface functionalization. The filament composite depicts the clear necking formation indicating the ductile behavior of the material. It is also observed that the elongation increases with increase in fluorine functionality and semi-ionic bonding. As the semi-ionic bonding of the filler decreases the tensile modulus and elongation break started to decrease for C-30 as filler.

The thermal and mechanical properties of the present work were compared with other reported thermoplastic filament composites and listed in Table 4. In some of the filament composites [35,42,49], the thermal properties either deteriorated or remain almost unchanged after addition of filler but there was an improvement in both the tensile modulus and tensile strength. Again, for those composites the mechanical properties improved up to a certain loading percentage and then decreased for higher filler loading %. The deterioration of mechanical properties for higher filler loading was attributed to the agglomeration filler particles in the polymer matrix. The loading percentage of filler also depends upon the particle size of the filler, if the particles size is too big the dispersion in polymer matrix will be difficult. A relatively higher percentage of filler loading i.e. 20, 40 and 60 % shows a reduction in tensile strength and elongation at break of the neat HDPE matrix [62]. Also, the interfacial adhesion of filler and polymer matrix can be improved by surface modification and other processes. Such as, the ultrasonicated biochar filler showed improved properties even in 0.75 % filler loading in comparison to the untreated one with high loading of 10 wt% [28]. Although there was no significant change in thermal properties, the mechanical properties improved in plasma treated hemp derived carbon as filler [42]. In the present work, both the thermal and mechanical properties were improved up to the optimized plasma treated carbon as filler.

Fig. 12 illustrates the fracture surface image of the neat polymer and filament composites after tensile test. For neat polymer, the fracture surface exhibits a fibrous pull out indicating the ductile behavior. The small particles observed in the neat polymer matrix are the inorganic additive added to the Walmart bag and these particles correspond to some calcium based materials (as confirmed from the elementary analysis by EDX and color mapping). As per the reported literature, calcium

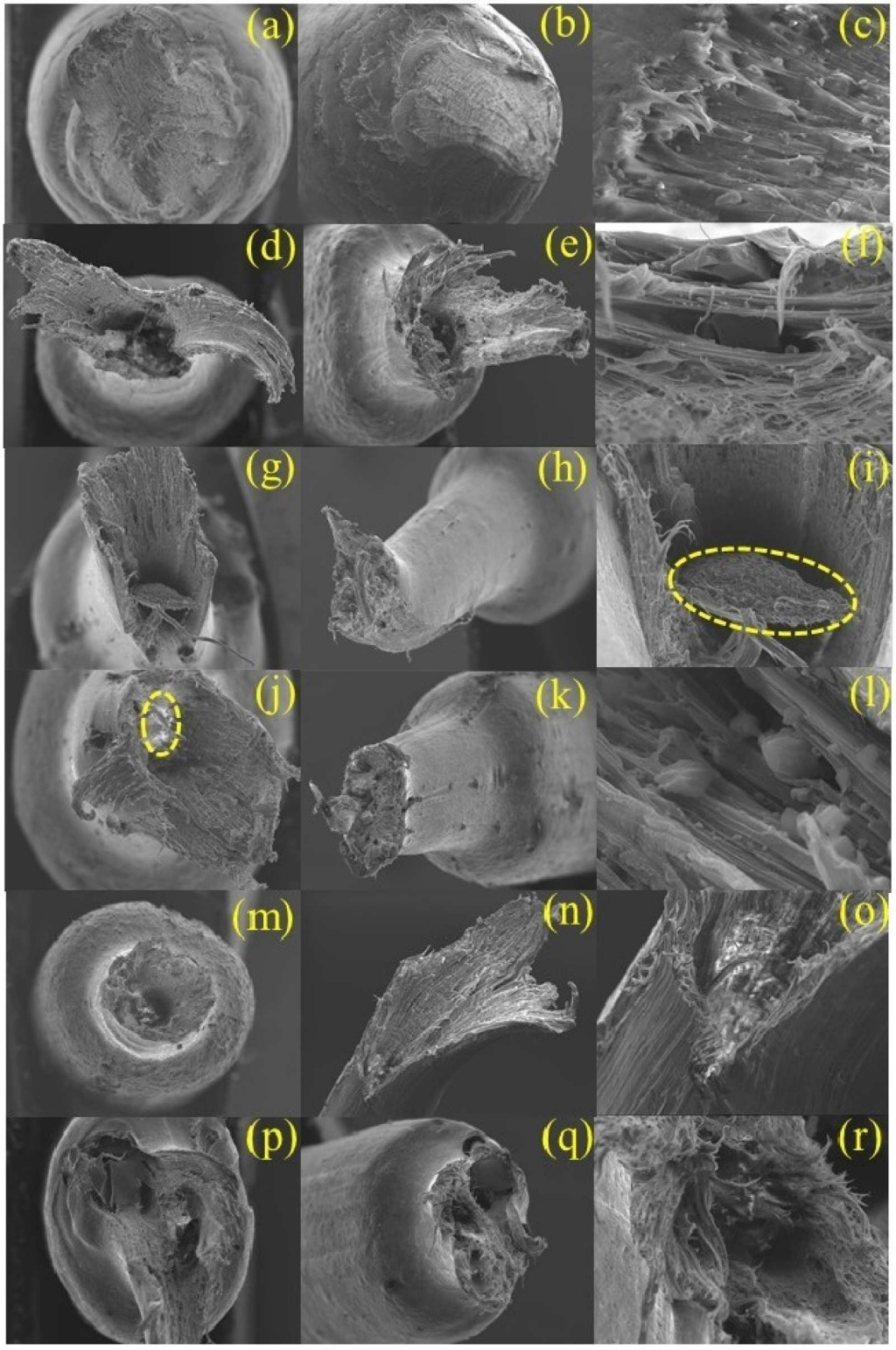

Fig. 12. Fracture surface of filament composites after tensile test: (a, b, c) WB (d, e, f) C-5 (g, h, i) C-10 (j, k, l) C-15 (m, n, o) C-20 (p, q, r) C-30.

carbonate ($CaCO_3$) generally added to plastic bags during the production process to enhance the usage properties like strength and elasticity [60]. Due to the addition of these inorganic additives, an additional decomposition observed in the TGA graph at temperature range of 630–700 °C similar to the reported literature [60]. As the filler added, the necking formation is more clear and more fibrous pull out observed. As shown in Fig. 13(i) and (j), 10 and 15 min plasma treated carbon particles completely coated with polymer matrix suggesting better interfacial adhesion between the filler and polymer. However, fracture surface analysis all the plasma treatment samples exhibit better interfacial adhesion with polymer matrix and yielding a difficult fracture with more fibrous pull out than the neat polymer.

Fig. 13. 3D printed sample of pure Walmart Bag filament.

3.2.3. *Printability test of filament composites*

A printability test was performed to check the application potentiality of the extruded filament for 3D printing applications. For preliminary testing, 3D printing of pure Walmart bag filament (HDPE) was carried out using a Hyrel 3D printing system with nozzle and bed temperature 250 °C and 100 °C, respectively. The printed part popped up from the base for the lower bed temperature range i.e. 80–95 °C. The bed temperature 100 °C was found to be the optimized temperature to bond the first layer with base. To get minimum warpage for the other layers, the chamber was closed to maintain the same temperature. The diameter of the filament used for the 3D printing was ~1.75 mm. A 5 cm* 5 cm square cube was printed with a printing speed of 60 mm/s and concentric infill type was used as shown in Fig. 13. 3D printing samples of the filament composites with ASTM standard will be printed and characterized in future research work. The present printing results emerged many opportunities for future studies.

4. Conclusion

This study explored the thermal and mechanical properties of SF_6 plasma treated spent coffee ground waste derived carbon reinforced waste HDPE filament composites, with a view to broaden its application potentiality in recently trending Material Extrusion 3D printing. The current investigation not only broaden the application potentiality but also involves a sustainable development of filament composites by integrating two major contributors of environmental issues and global warming i.e. spent coffee ground wastes and plastic waste (Walmart bag). Spent ground waste derived carbon are utilized as filler in the waste Walmart bag HDPE polymer matrix. In order to obtain a high-quality filler, the spent coffee ground derived carbon is treated with SF_6 plasma treatment. The fluorine functionalization of the pyrolyzed carbon can be controlled by plasma treatment time as observed from our investigations. XPS, FTIR and TGA analysis of the plasma treated carbon suggest the semi-ionic C-F bonding. It is observed that, up to a certain plasma treatment time i.e. 15 min, fluorine content is maximum leading to a maximum defect intensity confirmed from I_D/I_G ratio of the Raman spectra. After that, the fluorine content reduced due to breakdown of some of the less stabilized functional groups by further plasma treatment. This fluorine functionalization aid to enhance the thermal and mechanical properties of filament composite. The absence of active functional groups in untreated carbon as filler causes poor interaction between the filler and polymer matrix, hence the reduction of tensile modulus and tensile strength by 38.2 % and 5.7 % respectively than the neat HDPE matrix. The thermal stability of untreated carbon reinforced filament composites also decreased by 4 °C from the neat HDPE matrix. On the contrary, 15 min plasma treated carbon with highest fluorine functionalization as a filler exhibits 33.8 % and 13.97 % improvement in tensile modulus and tensile strength in comparison to neat HDPE matrix. The increase in thermal degradation temperature by 13 °C and 11 °C for 10 min and 15 min plasma treated carbon as filler indicates the enhanced thermal stability of the composites than the neat HDPE matrix. Initial attempt of printability test with composites reveals their potentiality in 3D printing application with some optimization in future studies. Apart from that, the plasma treated carbon reinforced filament composites with improved thermal and mechanical properties can be used in wide range of applications.

CRediT authorship contribution statement

Sushrisangita Sahoo: Investigation, Data curation, Conceptualization. **Abhinav Yadav:** Methodology, Investigation, Formal analysis, Data curation. **Vijaya Rangari:** Writing – review & editing, Supervision, Resources, Data curation, Conceptualization.

Declaration of competing interest

The authors declare the following financial interests/personal relationships which may be considered as potential competing interests:

Vijaya Rangari reports was provided by Tuskegee University. Vijaya Rangari reports a relationship with Tuskegee University College of Engineering that includes: employment. Sushrisangita Sahoo reports a relationship with Tuskegee University College of Engineering that includes: funding grants. Abhinav Yadav reports a relationship with Tuskegee University College of Engineering that includes:. All the authors are employed by Tuskegee University If there are other authors, they declare that they have no known competing financial interests or personal relationships that could have appeared to influence the work reported in this paper.

Funding Acknowledgment

The authors would like to acknowledge the constant financial support of NSF AL-EPSCoR #2148653, NSF-CREST #1735971.

Supplementary materials

Supplementary material associated with this article can be found, in the online version, at doi:10.1016/j.jcomc.2025.100570.

Data availability

Data will be made available on request.

References

[1] Agus Rimus Liandi Hendrawati, Mar'atus Solehah, Mohammad Herga Setyono, Isalmi Aziz, Yusraini Dian Inayati Siregar, Pyrolysis of PP and HDPE from plastic packaging waste into liquid hydrocarbons using natural zeolite Lampung as a catalyst, Case Stud. Chem. Environ. Eng. 7 (2023) 100290.
[2] Aymara Blanco, Rafael Juan, Robert Istrate, Beatriz Paredes, Mario Martin-Gamboa, Carlos Domínguez, Javier Dufour, Rafael A. García-Munoz, Assessing the circularity of post-consumer HDPE milk bottles through open-loop recycling and their environmental impact, Cleaner Environ. Syst. 13 (2024) 100185.
[3] Didem Civancik-Uslu, T.T. Nhu, Bart Van Gorp, Uros Kresovic, Macarena Larrain, Pieter Billen, Kim Ragaert, Steven De Meester, Jo Dewulf, Sophie Huysveld Resources, moving from linear to circular household plastic packaging in Belgium: prospective life cycle assessment of mechanical and thermochemical recycling, Conserv. Recyc. 171 (2021) 105633.
[4] LaShanda T.J. Korley, Thomas H. Epps, Brett A. Helms, Anthony J. Ryan, Toward polymer upcycling—Adding value and tackling circularity, Science (1979) 373 (2021) 66–69.
[5] Doris Knoblauch, Linda Mederake, Government policies combatting plastic pollution, Curr. Opin. Toxicol. 28 (2021) 87–96.
[6] Marvin Bachmann, Christian Zibunas, Jan Hartmann, Victor Tulus, Sangwon Suh, Gonzalo Guillén-Gosálbez, André Bardow, Towards circular plastics within planetary boundaries, Nat. Sustain. 6 (2023) 599–610.

[7] A.A. Cuadri, J.E. Martín-Alfonso, The effect of thermal and thermo-oxidative degradation conditions on rheological, chemical and thermal properties of HDPE, Polym. Degrad. Stab. 141 (2017) 11–18.

[8] L.A. Pinheiroa, M.A. Chinelattob, S.V. Canevarolo, The role of chain scission and chain branching in high density polyethylene during thermo-mechanical degradation, Polym. Degrad. Stab. 86 (2004) 445–453.

[9] Ganna Gryn'ova, Jennifer L. Hodgsona, Michelle L. Coote, Revising the mechanism of polymer autooxidation, Org. Biomol. Chem. 9 (2011) 480–490.

[10] Pavel Oblak, Joamin Gonzalez-Gutierrez, Barbara Zupancic, Alexandra Aulova, Igor Emri, Processability and mechanical properties of extensively recycled high density polyethylene, Polym. Degrad. Stab. 114 (2015) 133–145.

[11] Zoé O.G. Schyns, Michael P. Shaver, Mechanical recycling of packaging plastics: a review macromol, Rapid Commun 42 (2021) 2000415.

[12] Joachim Marisa, Sylvie Bourdonb, Jean-Michel Brossardb, Laurent Cauretc, Laurent Fontainea, Véronique Montembaul, Mechanical recycling: compatibilization of mixed thermoplastic wastes, Polym. Degrad. Stab. 147 (2018) 245–266.

[13] Coralie Jehanno, Irma Flores, Andrew P. Dove, Alejandro J. Müller, Fernando Ruipérez, Haritz Sardon, Organocatalysed depolymerisation of PET in a fully sustainable cycle using thermally stable protic ionic salt, Green. Chem. 20 (2018), 1205-121.

[14] Lihui Lua, Shogo Kumagaia, Tomohito Kamedaa, Ligang Luo, Toshiaki Yoshioka, Degradation of PVC waste into a flexible polymer by chemical modification using DINP moieties, RSC. Adv. 9 (2019) 28870–28875.

[15] J. Guapacha, E. M.Vallés, M.D. Failla, L.M. Quinzani, Efficiency of different chain-linking agents in the synthesis of long-chain branched polypropylene: molecular, thermal, and rheological characterization, Polym. Plast. Technol. Eng. 57 (12) (2017) 1209–1224.

[16] Seth Kane, Elisabeth Van Roijen, Cecily Ryan, Sabbie Mille, Reducing the environmental impacts of plastics while increasing strength: biochar fillers in biodegradable, recycled, and fossil-fuel derived plastics, Composites Part C: Open Access 8 (2022) 100253.

[17] Xiaolong Hao, Haiyang Zhou, Binshan Mu, Lei Chen, Qiong Guo, Xin Yi, Lichao Sun, Qingwen Wang, Rongxian Ou, Effects of fiber geometry and orientation distribution on the anisotropy of mechanical properties, creep behavior, and thermal expansion of natural fiber/HDPE composites, Composites Part B 185 (2020) 107778.

[18] Fabrizio Sarasinia, Jacopo Tirillòa, Claudia Sergia, Maria Carolina Seghinia, Luca Cozzarinib, Nina Graupner, Effect of basalt fibre hybridisation and sizing removal on mechanical and thermal properties of hemp fibre reinforced HDPE composites, Compos. Struct. 188 (2018), 394–40.

[19] Sumodh Kumar, Ramesh M. Ra, Mrityunjay Doddamani, Compressive behavior of 3D printed MWCNT/HDPE nanocomposites, Composites Communications 35 (2022) 101317.

[20] U. Atikler, D. Basalp, F. Tihminlioğlu, Mechanical and morphological properties of recycled high-density polyethylene, filled with calcium carbonate and fly ash, J. Appl. Polym. Sci. 102 (2006) 4460–4467.

[21] Adib Kalantar Mehrjerdi, Bijan Adl-Zarrabi, Sung-Woo Cho, Mikael Skrifvars, Mechanical and thermo-physical properties of high-density polyethylene modified with talc, J. Appl. Polym. Sci. 129 (2013) 2128–2138.

[22] U. Saeed, K. Hussain, G. Rizvi, HDPE reinforced with glass fibers: rheology, tensile properties, stress relaxation, and orientation of fibers, Polym. Compos. 35 (2014) 2159–2169.

[23] Thomas McGaurana, Nicholas Dunne, Beatrice M. Smytha, Eoin Cunningham, Incorporation of poultry eggshell and litter ash as high loading polymer fillers in polypropylene, Composites Part C: Open Access 3 (2020) 100080.

[24] Li Yan, Song Haoyuan, Qi Leijie, Zhen Guancheng, Liang Yuwei, Liu Xiaokun, Li Chunyang, Xie Qing, Modified lignin-based intumescent flame retardant's effect on flame retardancy, mechanical and electrical properties of HDPE material for cable sheathing, Polym. Test. 135 (2024) 108464.

[25] Dilpreet S. Bajwa, Sushil Adhikari, Jamileh Shojaeiarani, Sreekala G. Bajwa, Pankaj Pandey, Saravanan R. Shanmugam, Characterization of bio-carbon and ligno-cellulosic fiber reinforced bio-composites with compatibilizer, Constr. Build. Mater. 204 (2019) 193–202.

[26] Qingfa Zhang, Donghong Zhang, Hang Xu, Wenyu Lu, Xiajin Ren, Hongzhen Cai, Hanwu Lei, Erguang Huo, Yunfeng Zhao, Moriko Qian, Xiaona Lin, Elmar M. Villota, Wendy Mateo, Biochar filled high-density polyethylene composites with excellent properties: towards maximizing the utilization of agricultural wastes, Indust. Crops & Products 146 (2020) 11218.

[27] Seth Kane, Cecily Ryan, Biochar from food waste as a sustainable replacement for carbon black in upcycled or compostable composites, Composites Part C: Open Access 8 (2022) 100274.

[28] Zaheeruddin Mohammed, Shaik Jeelani, Vijaya Rangari, Effective reinforcement of engineered sustainable biochar carbon for 3D printed polypropylene biocomposites, Composites Part C: Open Access 7 (2022) 100221.

[29] Seth Kane, Elisabeth Van Roijen, Cecily Ryan, Sabbie Miller, Reducing the environmental impacts of plastics while increasing strength: biochar fillers in biodegradable, recycled, and fossil-fuel derived plastics, Composites Part C: Open Access 8 (2022) 100253.

[30] Qingfa Zhang, Donghong Zhang, Hang Xu, Wenyu Lu, Xiajin Ren, Hongzhen Cai, Hanwu Lei, Erguang Huo, Yunfeng Zhao, Moriko Qian, Xiaona Lin, Elmar M. Villota, Wendy Mateo, Biochar filled high-density polyethylene composites with excellent properties: towards maximizing the utilization of agricultural wastes, Industrial Crops & Products 146 (2020) 112185.

[31] Qingfa Zhang, Muhammad Usman Khan, Xiaona Lin, Hongzhen Cai, Hanwu Lei, Temperature varied biochar as a reinforcing filler for high-density polyethylene composites, Composites Part B 175 (2019) 107151.

[32] Tengku Yasim-Anuar Tengku Arisyah, Ng Yee-Foong Lawrence, Abdullahi Lawal Abubakar, Ahmad Farid Mohammed Abdillah, Mohd Yusuf Mohd Zulkhairi, Mohd Ali Hassan, Ariffin Hidayah, Emerging application of biochar as a renewable and superior filler in polymer composites, RSC. Adv. 12 (2022) 13938.

[33] Oisik Das, Debes Bhattacharyya, David Hui, Kin-Tak Lau, mechanical and flammability characterisations of biochar/polypropylene biocomposites, Composites Part B 106 (2016) 120–128.

[34] Mohanad Idrees, Shaik Jeelani, Vijaya Rangari, Three-dimensional-printed sustainable biochar-recycled PET composites, ACS Sustainable Chem. Eng. 6 (2018) 13940–13948.

[35] Nectarios Vidakis, Dimitrios Kalderis, Markos Petousis, Emmanuel Maravelakis, Nikolaos Mountakis, Nikolaos Bolanakis, Vassilis Papadakis, Biochar fller in MEX and VPP additive manufacturing: characterization and reinforcement efects in polylactic acid and standard grade resin matrices, Biochar. 5 (2023) 39.

[36] Qingfa Zhang, Li Yukang, Cai Hongzhen, Lin Xiaona, Yi Weiming, Zhang Jibing, Properties comparison of high density polyethylene composites filled with three kinds of shell fibers, Results. Phys. 12 (2019) 1542–1546.

[37] Peerayut Tapangnoi, Pongdhorn Sae-Oui, Weerawut Naebpetch, Chomsri Siriwong, Preparation of purified spent coffee ground and its reinforcement in natural rubber composite, Arab. J. Chem. 15 (2022) 103917.

[38] Congcan Shi, Yiyu Chen, Zhaohui Yu, Sheng Li, Huifang Chana, Shenghong Sun, Guangxue Chena, Minghui He, Junfei Tian, Sustainable and superhydrophobic spent coffee ground-derived holocellulose nanofibers foam for continuous oil/water separation, Sustain. Mater. Technol. 28 (2021) e00277.

[39] H. Kyung Lee, Y. Gi Park, T. Jeong, Y. Seok Song, Green nanocomposites filled with spent coffee grounds, J. Appl. Polym. Sci. 132 (2015) 42043.

[40] Martina Paramatti, Alessia Romani, Gianluca Pugliese, Marinella Levi, PLA feedstock filled with spent coffee grounds for new ProductApplications with large-format material extrusion additive manufacturing, ACS. Omega 9 (2024) 6423–6431.

[41] Mariana Marques, Luis F.F.F. Gonçalves, Carla I. Martins, Mario ' Vale, Fernando M. Duarte, Effect of polymer type on the properties of polypropylene composites with high loads of spent coffee grounds, Waste Management 154 (2022) 232–244.

[42] Gautam Chandrasekhar, Kearston Edwards, Desmond Mortley, Vijaya Rangari, Upcycling of waste polymer using surface modified hemp derived biochar carbon for sustainable packaging applications, ACS Sustain. Resour. Manage. 1 (2024) 625–633.

[43] Zaheeruddin Mohammed, Shaik Jeelani, Vijaya K. Rangari, Effect of low-temperature plasma treatment on starch-based biochar and its reinforcement for three-dimensional printed polypropylene biocomposites, ACS. Omega 7 (2022) 39636–39647.

[44] Hui Zhang, Liwei Fan, Huilong Dong, Pingping Zhang, Kaiqi Nie, Jun Zhong, Youyong Li, Jinghua Guo, Xuhui Sun, Spectroscopic investigation of plasma-fluorinated monolayer graphene and application for gas sensing, ACS Appl. Mater. Interfaces 8 (2016) 8652–8661.

[45] Lyubov G. Bulusheva, Yuliya V. Fedoseeva, Emmanuel Flahaut, Jérémy Rio, Christopher P. Ewels, Victor O. Koroteev, Gregory Van Lier, Denis V. Vyalikh, Alexander V. Okotrub, Effect of the fluorination technique on the surface-fluorination patterning of double-walled carbon nanotubes, Beilstein J. Nanotechnol. 8 (2017) 1688–1698.

[46] Paola Brachi, Victor Santes, Enelio Torres-Garcia, Pyrolytic degradation of spent coffee ground: a thermokinetic analysis through the dependence of activation energy on conversion and temperature, Fuel 302 (2021) 120995.

[47] Randeep Gabhi, Luca Basile, Donald W. Kirk, Mauro Giorcelli, Alberto Tagliaferro, Charles Q. Jia, Electrical conductivity of wood biochar monoliths and its dependence on pyrolysis temperature, Biochar. 2 (2020) 369–378.

[48] Akash Roshan, Dipita Ghosh, Subodh Kumar Maiti, How temperature affects biochar properties for application in coal mine spoils? A meta-analysis, Carbon Research 2 (2023) 1–17.

[49] Chibu O. Umerah, Deepa Kodali, Sydnei Head, Shaik Jeelani, Vijaya K. Rangari, Synthesis of carbon from waste coconut shell and their application as filler in bioplast polymer filaments for 3D printing, Composites Part B 202 (2020) 108428.

[50] Deepa Kodali, Chibu O Umerah, Mohanad O Idrees, S. Jeelani, Vijaya K Rangari, Fabrication and characterization of polycarbonate-silica filaments for 3D printing applications, J. Compos. Mater. 55 (2021) 1–10.

[51] Vinay Gupta, Tsuyoshi Nakajima, Yoshimi Ohzawa, Boris Z emv, A study on the formation mechanism of graphite fluorides by Raman spectroscopy, J. Fluor. Chem. 120 (2003) 143–150.

[52] Kingsley K.C. Ho, Graham Beamson, George Shia, Natalya V. Polyakova, Alexander Bismarck, Surface and bulk properties of severely fluorinated carbon fibres, J. Fluor. Chem. 128 (2007) 1359–1368.

[53] Rohit Yadav, Prerna Joshi, Masanori Hara, Masamichi Yoshimu, In situ electrochemical Raman investigation of charge storage in rGO and N-doped rGO, Phys. Chem. Chem. Phys. 23 (2021) 11789–11796.

[54] Xu Wang, Weimiao Wang, Yang Liu, Mengmeng Ren, Huining Xiao, Xiangyang Liu, Characterization of conformation and locations of C−F bonds in graphene derivative by polarized ATR-FTIR, Anal. Chem. 88 (2016) 3926–3934.

[55] V. Gupta, R.B. Mathur, O.P. Bahl, A. Tressaud, S. Flandrois, Thermal stability of Fluorine intercalated carbon fibers, Synthetic metal 73 (1995) 69–75.

[56] Amita Shakya, Meththika Vithanage, Tripti Agarwal, Influence of pyrolysis temperature on biochar properties and Cr(VI) adsorption from water with groundnut shell biochars: mechanistic approach, Environ. Res. 215 (2022) 114243.

[57] Jean-Charles Agopian, Olivier Teraube, Karine Charlet, Samar Hajjar-Garreau, Elodie Petit, Nicolas Batisse, Marc Dubois, Carbon fibre fluorination: surface and structural properties, Appl. Surf. Sci. 595 (2022) 153561.
[58] Na Lu, Shubhashini Oza, Thermal stability and thermo-mechanical properties of hemp-high density polyethylene composites: effect of two different chemical modifications, Composites: Part B 44 (2013) 484–490.
[59] Rossella Arrigo, Mattia Bartoli, GiulioMalucelli, Poly(lactic Acid)–Biochar biocomposites: effect of processing and filler content on rheological, thermal, and mechanical properties, Polymers. (Basel) 12 (2020) 892.
[60] Xiaoli Zhou, Pinjing He, Wei Peng, Fan Lü, Liming Shao, Hua Zhang, Upcycling of real-world HDPE plastic wastes into high-purity methane and hierarchical porous carbon materials: influence of plastics additives, J. Environ. Chem. Eng. 11 (2023) 109327.
[61] A.U. Chaudhry, Sunil P. Lonkar, Ratiram G. Chudhary, Abdelnasser Mabrouk, Ahmed A. Abdala, Thermal, electrical, and mechanical properties of highly filled HDPE/graphite nanoplatelets composites, Materials Today: Proceedings 29 (2020) 704–708.
[62] H.S. Bharath, Dileep Bonthu, Pavana Prabhakar, Mrityunjay Doddamani, Three-dimensional printed lightweight composite foams, ACS. Omega 5 (2020) 22536–22550.